energies

MDPI

Article

Impedance Compensation Method Considering Unbalanced Ground Fault with SFCL in a Power Distribution System

Yoo-Jung Cho and Sung-Hun Lim *

Department of Electrical Engineering, Soongsil University, 369, Sangdo-ro, Dongjak-gu, Seoul 156-743, Korea
* Correspondence: superlsh73@ssu.ac.kr

Abstract: As the energy demand increases due to the developing electric power industry, the fault current becomes higher during the fault time. A new approach is needed to reduce a fault current in a power distribution system, since the fault currents influence other protective devices' operation. To decrease the fault current, the superconducting fault current limiter (SFCL) has been suggested. The SFCL has no power loss with no effect on a power distribution system because the SFCL impedance only occurs during the fault time. However, the SFCL can reduce the fault current; it causes the trip time delay of the over current relay (OCR). Compensation methods for the balanced fault have been invented in previous studies, while research on unbalanced ground fault compensation are few. In this paper, the compensation method configured with impedance components of a power distribution system is introduced to eliminate the influence of the SFCL on the OCR. In addition, the components of the SFCL impedance are removed from the characteristic equation of the OCR. To verify the effect of the impedance compensation method, fault simulations are carried out in 3 types of ground faults using PSCAD/EMTDC.

Keywords: over current relay (OCR); superconducting fault current limiter (SFCL); impedance components; impedance compensation method; power distribution system

Citation: Cho, Y.-J.; Lim, S.-H. Impedance Compensation Method considering Unbalanced Ground Fault with SFCL in a Power Distribution System. *Energies* **2022**, *15*, 7405. https://doi.org/10.3390/en15197405

Academic Editor: Ferdinanda Ponci

Received: 18 August 2022
Accepted: 7 September 2022
Published: 9 October 2022

1. Introduction

The energy demand of a power system increases due to the development of the electric power industry and the complexity of a power system. As a result, the fault current increases and power devices exceed their capacities and their operation is affected. It is necessary to increase the capacity of devices in a power distribution system to reduce the fault current, but it is economically burdensome.

Another way to limit the increasing fault current is by installing a superconducting fault current limiter (SFCL). The SFCL is economical in that it has no loss and quickly limits the fault current in a power distribution system by the quench occurrence of the high temperature superconducting (HTSC) element. In normal operation, the resistance of the HTSC element is zero; the SFCL has no effect on a power distribution system. If the fault occurs, the resistance of the HTSC element obtains a value and performs the fast fault current limiting operation. Different types of the SFCLs exist, such as typically resistive-type, transformer-type, flux-lock-type, hybrid type and trigger-type SFCL. The trigger-type SFCL has the advantage of minimizing the power consumption of the HTSC element by using a switching operation [1–8].

Though the SFCL effectively controls the fault current, the SFCL obstructs the activation of the OCR. The OCR has inverse characteristics for the fault current, so the trip time of the OCR is delayed as the fault current decreases due to the SFCL. The trip delay problem of the OCR (due to the fault current limiting operation of the SFCL) has been found, in many previous studies, to be resolved by resetting the characteristic equation of the OCR using the current or voltage components. However, these previous reports only

deal with balanced ground fault situations and may cause malfunction in unbalanced ground faults, since the fault current is different in each ground fault. All ground types of faults must be considered because unbalanced ground fault such as single-line and double-line ground faults (SLG, DLG) occur more than balanced ground faults such as triple-line ground faults (TLG) [9–21].

In this paper, the impedance compensation method for the OCR using power distribution system components are suggested to lessen the effect of the SFCL. Research on balanced ground faults were suggested in previous studies, so the impedance compensation method for unbalanced ground fault is investigated. To prove the impedance compensation method for the OCR operation, it is derived through the simulation comparison by Power Systems Computer Aided Design (PSCAD) and Electro Magnetic Transient DC analysis program (EMTDC).

2. Configuration of Power Distribution System with SFCL

2.1. Structure of Power Distribution System

A power distribution system, simulated in Figure 1, consists of a single feeder line, source, main transformer (MTR), loads, the over current relay (OCR), the circuit breaker (CB) and trigger-type SFCL. The OCR measures three phase feeder currents through the current transformer (CT), and three phase feeder voltages and the SFCL voltages in three phases are estimated by the potential transformer (PT). After that, three phase currents and voltages are changed into the sequence components (positive, negative, zero). The OCR controls the CB using sequence components of feeder currents against the fault situation. These sequence components of feeder currents and voltages are used to derive the sequence impedance components, which are applied to the impedance compensation method of the OCR described in Section 3.2. In addition, a load of 5 [MW] (Z_{Load}) is installed at the end point of the feeder. The feeder lines (Z_{Line}) have resistance and reactance in each phase, and conductance is set very low to omit the mutual impedance, since it affects the formation of the impedance compensation method. The three types of ground fault, which are the single-line ground fault (SLG), double-line ground fault (DLG) and the triple-line ground fault (TLG), emerge at the 10 [km] point from the feeder. One of the three ground faults occurs and has different results, as shown in Section 4. Specifications of power distribution system are shown in Table 1 [22].

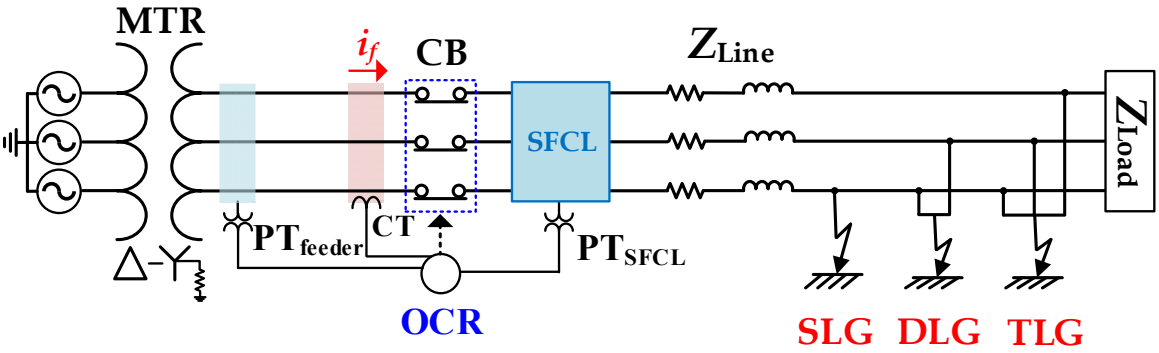

Figure 1. Structure of power distribution system with superconducting fault current limiter (SFCL).

Table 1. Specifications of Power Distribution System.

Experimental Circuit	Value	Unit
Source	154	[kV]
	100	[MVA]
MTR	154/22.9	[kV]
	60	[MVA]

Line Impedance	ZP = ZN = 0.182 + j0.391 Z0 = 0.518 + j1.189	[Ω/km] [Ω/km]
Feeder Length	10	[km]
Load	5 PF = 0.95	[MW]

2.2. Trigger Type SFCL Modeling

Figure 2 shows three phase trigger type SFCL, which controls the fault current by activating the breaker with the control circuit. The control circuit measures the voltage of the high temperature superconducting (HTSC) element (V_{SC}) and the current (I_{CLR}) of the current limiting reactor (CLR). Then, the control circuit sends a close/open signal to the breaker. In normal operation, the current only flows into the HTSC element since it is zero resistance. When the fault occurs, the fault current exceeds the critical current (I_C) and the resistance of the HTSC element obtains a value. If the voltages of the HTSC element (V_{SC}) exceed the setting voltage (V_{Set}), the control circuit makes a signal to open the breaker and the fault current flows into the CLR due to the opening of the breaker. If the CLR current decreases more than the setting current (I_{Set}) after the fault disappears, the control circuit sends a signal to close the breaker and the current again flows into the HTSC element by the closing operation of the breaker. Therefore, trigger-type SFCL is an economic model due to the trigger operation with the HTSC element and the control circuit. To improve the trip time delay of OCR, a suggested impedance compensation method will be used with the SFCL. Detailed parameters of trigger type SFCL are described in Table 2.

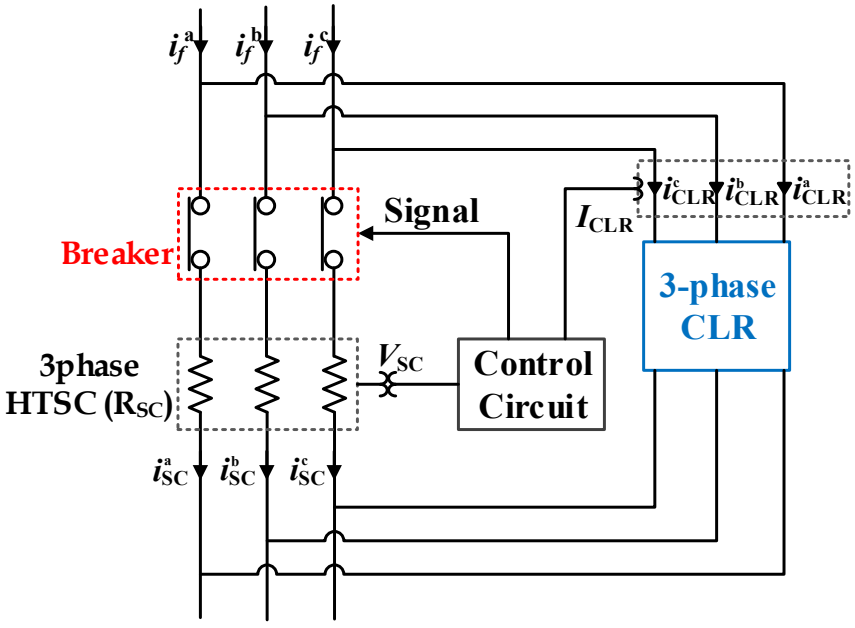

Figure 2. Configuration of trigger type SFCL.

Table 2. Parameters of trigger type SFCL.

Parameters	Value	Unit
V_{Set}	1	[kV]
I_{Set}	0.5	[kA]
HTSC	Convergence resistance (R_n) = 5 Critical current (I_C) = 1	[Ω] [kA]
CLR	j1.6	[Ω]

3. Operational Characteristic of over Current Relay

3.1. Equivalent Impedance of Power Distribution System

The equivalent impedance of a power distribution system is represented in the matrix to discuss the effect of the SFCL on a power distribution system. The impedance matrix equations are presented in 3 cases of the ground fault:

1. Case 1: Single-line ground fault (SLG)
2. Case 2: Double-line ground fault (DLG)
3. Case 3: Triple-line ground fault (TLG)

The impedance matrix equations are expressed in the sequence components $\left(Z_{feeder}^{0PN}\right)$ and three phases' components $\left(Z_{feeder}^{abc}\right)$. In normal operation, three phase and sequence impedance matrix equations are shown in (1).

$$Z_{feeder}^{abc} = Z_{feeder}^{0PN} = \begin{bmatrix} Z_{line} + Z_{load} & 0 & 0 \\ 0 & Z_{line} + Z_{load} & 0 \\ 0 & 0 & Z_{line} + Z_{load} \end{bmatrix} \quad (1)$$

Z_{line} is the line impedance and Z_{load} is the load impedance described in Figure 1. A main diagonal of Z_{feeder}^{abc} is three phase feeder impedance and Z_{feeder}^{0PN} main diagonal called the self-impedance is the sequence components of the feeder impedances. An off diagonal of $Z_{feeder}^{abc}$and Z_{feeder}^{0PN} are the mutual impedances and they are all zero-value, as described in Section 2.1. These two impedance matrix equations are the same before the fault period. After the fault occurs, $Z_{feeder}^{abc}$and Z_{feeder}^{0PN} are expressed in 3 cases on the ground fault type.

Case 1, the single-line ground fault (SLG) occurs in the a-phase, Z_{load} disappears in a faulted phase and the SFCL impedances (Z_{SFCL}) are added in each phase at Z_{feeder}^{abc} shown in (2). Z_{feeder}^{abc} is converted to Z_{feeder}^{0PN} by using the convert Equations (3) and (4).

$$Z_{feeder}^{abc} = \begin{bmatrix} Z_{line} + Z_{SFCL} & 0 & 0 \\ 0 & Z_{line} + Z_{load} + Z_{SFCL} & 0 \\ 0 & 0 & Z_{line} + Z_{load} + Z_{SFCL} \end{bmatrix} \quad (2)$$

$$A = \begin{bmatrix} 1 & 1 & 1 \\ 1 & a^2 & a \\ 1 & a & a^2 \end{bmatrix}, a = 1\angle 120^\circ \quad (3)$$

$$Z^{0PN} = A^{-1} Z^{abc} A \quad (4)$$

Z_{feeder}^{0PN} is shown in (5) derived from (2) to (4). In (5), only a main diagonal of Z_{feeder}^{0PN} has the Z_{SFCL}, whereas an off diagonal has only the load impedances. A main diagonal is the self impedance and off diagonal is the mutual impedance. As seen in (5), the SFCL only affects the main diagonal called the self-impedance in a power distribution system.

$$Z_{feeder}^{0PN} = \frac{1}{3}\begin{bmatrix} 3(Z_{line} + Z_{SFCL}) + 2Z_{load} & -Z_{load} & -Z_{load} \\ -Z_{load} & 3(Z_{line} + Z_{SFCL}) + 2Z_{load} & -Z_{load} \\ -Z_{load} & -Z_{load} & 3(Z_{line} + Z_{SFCL}) + 2Z_{load} \end{bmatrix} \quad (5)$$

Case 2, the double-line ground fault (DLG) appears in the ab-phase, Z_{load} disappears from the faulted phase and Z_{SFCL} is added in each phase shown in (6). Z_{feeder}^{0PN} shown in (7) is derived from (6) and the convert Equations (3) and (4).

$$Z_{feeder}^{abc} = \begin{bmatrix} Z_{Line} + Z_{SFCL} & 0 & 0 \\ 0 & Z_{Line} + Z_{SFCL} & 0 \\ 0 & 0 & Z_{Line} + Z_{Load} + Z_{SFCL} \end{bmatrix} \quad (6)$$

$$Z_{feeder}^{0PN} = \frac{1}{3}\begin{bmatrix} 3(Z_{line} + Z_{SFCL}) + Z_{load} & aZ_{load} & a^2 Z_{load} \\ a^2 Z_{load} & 3(Z_{line} + Z_{SFCL}) + Z_{load} & aZ_{load} \\ aZ_{load} & a^2 Z_{load} & 3(Z_{line} + Z_{SFCL}) + Z_{load} \end{bmatrix} \quad (7)$$

Case 3, when the triple-line ground fault (TLG) occurs, Z_{load} is disappeared and Z_{SFCL} is added in all phases, described in (8). Z_{feeder}^{abc} and Z_{feeder}^{0PN} are identical in TLG.

$$Z_{feeder}^{abc} = \begin{bmatrix} Z_{line} + Z_{SFCL} & 0 & 0 \\ 0 & Z_{line} + Z_{SFCL} & 0 \\ 0 & 0 & Z_{line} + Z_{SFCL} \end{bmatrix} \tag{8}$$

$$Z_{feeder}^{0PN} = \begin{bmatrix} Z_{line} + Z_{SFCL} & 0 & 0 \\ 0 & Z_{line} + Z_{SFCL} & 0 \\ 0 & 0 & Z_{line} + Z_{SFCL} \end{bmatrix} \tag{9}$$

From (5), (7) and (9), the sequence impedance component of the SFCL includes in a diagonal elements of Z_{feeder}^{0PN}, consequently the SFCL impedance (Z_{SFCL}) affects only the sequence self-impedances (positive, negative, zero) of the feeder line. On this basis, the impedance compensation method of the OCR can be composed only of the sequence self-impedance components of the feeder line. The sequence impedance matrixes are different according to the ground fault type, the impedance compensation method should be different on each ground fault [23–27].

3.2. Over Current Relay's Characteristic Modeling

The operation of the OCR is described by a characteristic equation with inverse characteristics shown in (10) to (12). *TD* is a time dial of the OCR, M_I is an operation indicator value and *A*, *B*, and *p* are constants referred to KEPCO's (Korea Electric Power Corporation) OCR Standard. M_I is the ratio of feeder current (I_f) divided into setting current (I_{pickup}). I_f indicates the sum of the feeder current's phasor sequence components and I_{pickup} is the pickup current considering rated voltage and line capacities. If the SFCL operates on the feeder, I_f is reduced and the trip time of OCR is delayed. The zero and negative sequences of the feeder current (I_f^0, I_f^N) are zero at the triple line ground fault (TLG) [16,28].

$$T_{trip} = TD\left(\frac{A}{M^p - 1} + B\right) \tag{10}$$

$$M_I = \frac{I_f}{I_{pickup}} \tag{11}$$

$$I_f = \left|I_f^0 + I_f^P + I_f^N\right| \tag{12}$$

Therefore, the compensation method is needed to minimize the influence of the SFCL. (13) to (15) form the equations of the sequence impedance by reflecting the sequence feeder voltage (V_{feeder}) and pickup voltage (V_{pickup}). The zero and negative sequences of the feeder voltage (V^0_{feeder}, V^N_{feeder}) are zero at the triple-line ground fault (TLG).

$$M_{IV}^0 = \frac{I_f^0}{I_{pickup}}\left(\frac{KV_{pickup}}{V_{feeder}^0}\right) = \frac{KZ_{pickup}}{Z_{feeder}^0} \tag{13}$$

$$M_{IV}^P = \frac{I_f^P}{I_{pickup}}\left(\frac{KV_{pickup}}{V_{feeder}^P}\right) = \frac{KZ_{pickup}}{Z_{feeder}^P} \tag{14}$$

$$M_{IV}^N = \frac{I_f^N}{I_{pickup}}\left(\frac{KV_{pickup}}{V_{feeder}^N}\right) = \frac{KZ_{pickup}}{Z_{feeder}^N} \tag{15}$$

(13) to (15) are converted into the reciprocals, then all reciprocal equations are added together and converted into the reciprocal again to make the sequence impedance Equation (16).

$$M_{IV} = \frac{1}{\frac{1}{M_{IV}^0} + \frac{1}{M_{IV}^P} + \frac{1}{M_{IV}^N}} = \frac{KZ_{pickup}}{Z_{feeder}^0 + Z_{feeder}^P + Z_{feeder}^N} = \frac{KZ_{pickup}}{\left|\begin{matrix}\left(R_{feeder}^0 + jX_{feeder}^0\right) + \left(R_{feeder}^P + jX_{feeder}^P\right) \\ +\left(R_{feeder}^N + jX_{feeder}^N\right)\end{matrix}\right|} \quad (16)$$

In (16), the sequence impedances of the SFCL should be eliminated from the feeder impedances to remove the effect of the SFCL from OCR's trip operation. (17) is the impedance compensation method that the compensation constant *K* changes the result of (17) depending on the ground fault type. The parameters of OCR are described in Table 3.

$$M_Z^{0PN} = \frac{KZ_{pickup}}{\left|\begin{matrix}\left(R_{feeder}^0 - R_{SFCL}^0\right) + j\left[\left(X_{feeder}^0 - X_{SFCL}^0\right)\right] \\ +\left(R_{feeder}^P - R_{SFCL}^P\right) + j\left[\left(X_{feeder}^P - X_{SFCL}^P\right)\right] \\ +\left(R_{feeder}^N - R_{SFCL}^N\right) + j\left[\left(X_{feeder}^N - X_{SFCL}^N\right)\right]\end{matrix}\right|} \quad (17)$$

Table 3. Parameters of OCR.

Parameters	Data
TD	0.1
A	39.85
B	1.084
p	1.95
V_{pickup} [kV]	10.56
I_{pickup} [kA]	0.504

The flowchart of the impedance compensation method with the OCR operational algorithm is shown in Figure 3. The ground fault type is determined by measuring the resistance occurrence of HTSC element in each phase. After that, *Mz* is calculated using the sequence components of the feeder voltages, the SFCL voltages and the feeder currents. *Mz* is progressed with the operating characteristic of the OCR (10).

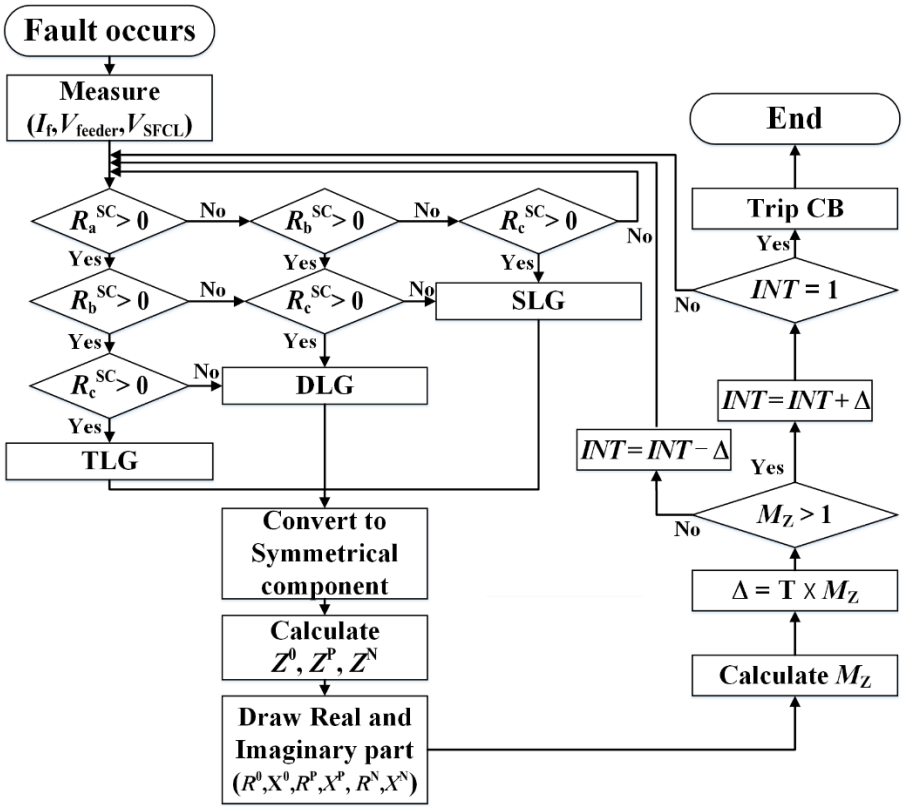

Figure 3. OCR operational algorithm flowchart.

4. Results and Discussion

Fault current limiting of the over-current relay (OCR) using the impedance compensation method was analyzed from the simulation results in three types of ground fault. The fault simulations were performed in two OCR characteristic equations, which were the existing OCR algorithm (2) and the impedance compensation method (17). After that, the results with the SFCL were compared. In addition, three results of the impedance compensation method (17) were analyzed according to different *K* values (1, 2, and 3.5). Three types of ground faults were simulated in 0.3 [s] to analyze the results of the OCR's operation.

4.1. Single-Line Ground Fault

Figure 4 shows the single-line ground fault (SLG) in a phase to ground using the existing over-current relay (OCR) algorithm (2). OCR operates at 0.882 [s] without the SFCL and OCR with SFCL operates at 1.083 [s]. Figure 4a shows the feeder voltage and currents when the SFCL is installed. The operation of OCR using (2) is expressed in the integration value INT_I, which increases after the fault occurs. The OCR is tripped when INT_I approaches "1" point as seen in Figure 4b, which activates the CB to be open and separates the fault section from the main grid. In Figure 4c, the resistance of HTSC element (R^a_{SC}) obtains a resistance value because the fault current (I_f) exceeds the critical current. During the fault time, the voltage of the SFCL (v_{SFCL}) is reduced by R^a_{SC} and increased again since the direction of the fault current changes to the current limiting reactor (CLR). Figure 4d shows the sequence component waveforms of the feeder voltages and currents. The dotted line is the feeder voltage and current using existing the OCR algorithm (2) without the SFCL and the solid line is the identical condition with the SFCL. The zero and negative sequence feeder voltages are almost the same. Figure 4e is the sequence component waveforms of the feeder impedances. The dotted line is the feeder impedances using the existing OCR algorithm (2) without the SFCL and the solid line is the identical condition

with the SFCL. Figure 4f is the sequence component waveform of the SFCL voltages and impedances.

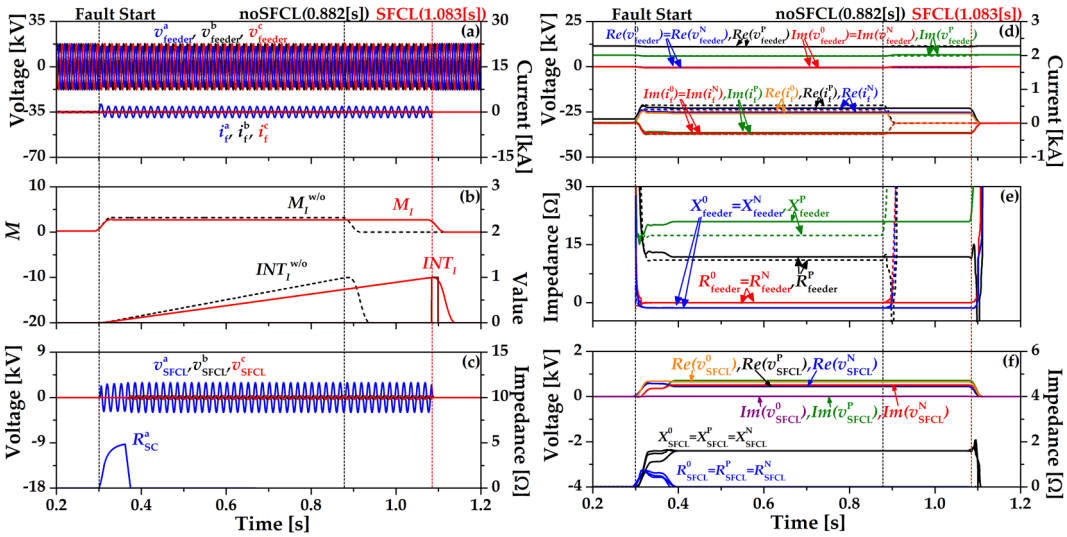

Figure 4. Waveforms and signals of OCR using M_I in SLG. (**a**) Three phase feeder voltage (v_{feeder}), current (i_f). (**b**) Index of CB (M_I) and signal of OCR (INT_I). (**c**) Three phase SFCL voltage (v_{SFCL}), HTSC element (R^a_{SC}). (**d**) Sequence feeder voltages (v^0_{feeder}, v^P_{feeder}, v^N_{feeder}), sequence feeder currents (i^0_f, i^P_f, i^N_f). (**e**) Sequence feeder impedances (R^0_{feeder}, R^P_{feeder}, R^N_{feeder}, X^0_{feeder}, X^P_{feeder}, X^N_{feeder}). (**f**) Sequence SFCL voltages (v^0_{SFCL}, v^P_{SFCL}, v^N_{SFCL}) and sequence SFCL impedances (R^0_{SFCL}, R^P_{SFCL}, R^N_{SFCL}, X^0_{SFCL}, X^P_{SFCL}, X^N_{SFCL}).

Figure 5 shows the single-line ground fault (SLG) in a phase to ground using the impedance compensation method (17). In Figure 5b, the operation of OCR using (17) is expressed in the integration value INT_Z, which has three different waveforms depending on K values (1, 2, 3.5). When K = 3.5, the index value (M_Z) and INT_Z are most similar to the existing OCR algorithm (2) without SFCL ($INT^{w/o}_I$). OCR operates at 0.88 [s] and decreased by 0.002 [s] compared to the existing OCR algorithm (2) with SFCL. In Figure 5c, resistance of the HTSC element (R^a_{SC}) is the same as Figure 4 since the breaker operation of the SFCL is constant as the critical current (I_C) is maintained. During the fault time, the voltage of the SFCL (v_{SFCL}) is reduced by R^a_{SC} and increased again since the direction of the fault current changes to the current limiting reactor (CLR). Figure 5d shows the sequence components' waveforms of the feeder voltages and currents. The dotted line is the feeder voltages and currents using existing OCR algorithm (2) without the SFCL and the solid line is the impedance compensation method (17) with the SFCL. The zero and negative sequence feeder voltages are almost the same. Figure 5e is the sequence components' waveforms of feeder impedance. The dotted line is the feeder impedances using the existing OCR algorithm (2) without the SFCL and the solid line is the feeder impedances using the impedance compensation method (17) with the SFCL. Figure 5f is the sequence component waveforms of the SFCL voltages and impedances.

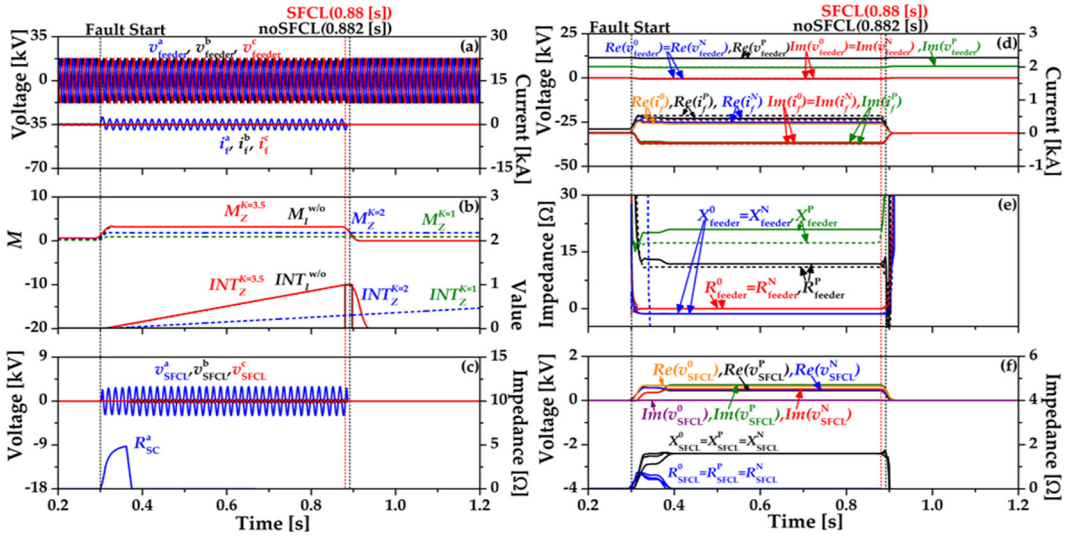

Figure 5. Waveforms and signals of OCR using M_I, M_Z in SLG. (**a**) Three phase feeder voltage (v_{feeder}), current (i_f). (**b**) Index of CB (M_I, M_Z) and signal of OCR (INT_I, INT_Z). (**c**) Three phase SFCL voltage (v_{SFCL}), HTSC element (R^a_{SC}). (**d**) Sequence feeder voltages (v^0_{feeder}, v^P_{feeder}, v^N_{feeder}), sequence feeder currents (i^0_f, i^P_f, i^N_f). (**e**) Sequence feeder impedances (R^0_{feeder}, R^P_{feeder}, R^N_{feeder}, X^0_{feeder}, X^P_{feeder}, X^N_{feeder}). (**f**) Sequence SFCL voltages (v^0_{SFCL}, v^P_{SFCL}, v^N_{SFCL}) and sequence SFCL impedances (R^0_{SFCL}, R^P_{SFCL}, R^N_{SFCL}, X^0_{SFCL}, X^P_{SFCL}, X^N_{SFCL}).

4.2. Double-Line Ground Fault

Figure 6 shows the double-line ground fault (DLG) in ab phase to ground using the existing over-current relay (OCR) algorithm (2). OCR operates at 0.669 [s] without the SFCL and OCR with SFCL operates at 0.811 [s]. Figure 6a shows the feeder voltages and currents when the SFCL is installed. The operation of OCR using (2) is expressed in the integration value INT_I, which increases after the fault occurs and when INT_I approaches "1" point as seen in Figure 6b. In Figure 6c, resistance of HTSC element (R^a_{SC}, R^b_{SC}) obtains a resistance value because the fault current (I_f) exceeds the critical current and R^a_{SC}, R^b_{SC} becomes zero when the breaker in the SFCL is operated, as explained in Section 2.2. During the fault time, the voltage of the SFCL (v_{SFCL}) is reduced by R^a_{SC} and increased again since the direction of the fault current changes to the current limiting reactor (CLR). Figure 6d shows the sequence components' waveforms of the feeder voltages and currents. The dotted line is the feeder voltages and currents using the existing OCR algorithm (2) without the SFCL and the solid line is the identical condition with the SFCL. The zero and negative sequence feeder voltages are almost the same. Figure 6e shows the sequence components' waveforms of feeder impedances. The dotted line is the feeder impedances using the existing OCR algorithm (2) without the SFCL and the solid line is the identical condition with the SFCL. Figure 6f is the sequence component waveforms of the SFCL voltages and impedances.

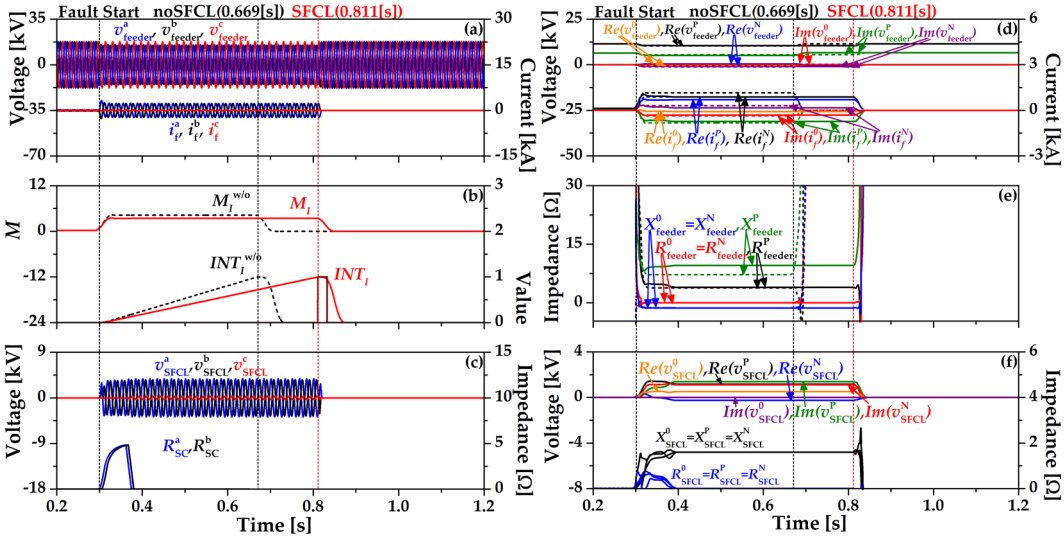

Figure 6. Waveforms and signals of OCR using M_I in DLG. (**a**) Three phase feeder voltage (v_{feeder}), current (i_f). (**b**) Index of CB (M_I) and signal of OCR (INT_I). (**c**) Three phase SFCL voltage (v_{SFCL}), HTSC element (R^a_{SC}, R^b_{SC}). (**d**) Sequence feeder voltages (v^0_{feeder}, v^P_{feeder}, v^N_{feeder}), sequence feeder currents (i^0_f, i^P_f, i^N_f). (**e**) Sequence feeder impedances (R^0_{feeder}, R^P_{feeder}, R^N_{feeder}, X^0_{feeder}, X^P_{feeder}, X^N_{feeder}). (**f**) Sequence SFCL voltages (v^0_{SFCL}, v^P_{SFCL}, v^N_{SFCL}) and sequence SFCL impedances (R^0_{SFCL}, R^P_{SFCL}, R^N_{SFCL}, X^0_{SFCL}, X^P_{SFCL}, X^N_{SFCL}).

Figure 7 shows the double-line ground fault (DLG) in ab phase to ground using impedance compensation method (17). In Figure 7b, the operation of OCR using (17) is expressed in the integration value INT_Z, which has three different waveforms depending on the K value (1, 2, 3.5). When K = 2, index value (M_Z) and INT_Z are most similar to the existing OCR algorithm (2) without SFCL ($INT^{w/o}_I$). OCR operates at 0.666 [s] and decreased by 0.14 [s] compared to the existing OCR algorithm (2) with SFCL. In Figure 5c, the resistance of the HTSC element (R^a_{SC}, R^b_{SC}) is same with Figure 6 since the breaker operation is constant as the critical current (I_C) is maintained. During the fault time, voltage of the SFCL (v_{SFCL}) is reduced by R^a_{SC}, R^b_{SC} and increased again since the direction of the fault current changes to the current limiting reactor (CLR). Figure 7d shows the sequence components waveforms of the feeder voltages and currents. The dotted line is the feeder voltages and currents using the existing OCR algorithm (2) without the SFCL and the solid line is the impedance compensation method (17) with the SFCL. The zero and negative sequence voltages are almost the same. Figure 7e is the sequence components waveforms of feeder impedances. The dotted line is the feeder impedances using the existing OCR algorithm (2) without the SFCL and the solid line is the feeder impedances using the impedance compensation method (17) with the SFCL. Figure 7f is the sequence component waveforms of the SFCL voltages and impedances.

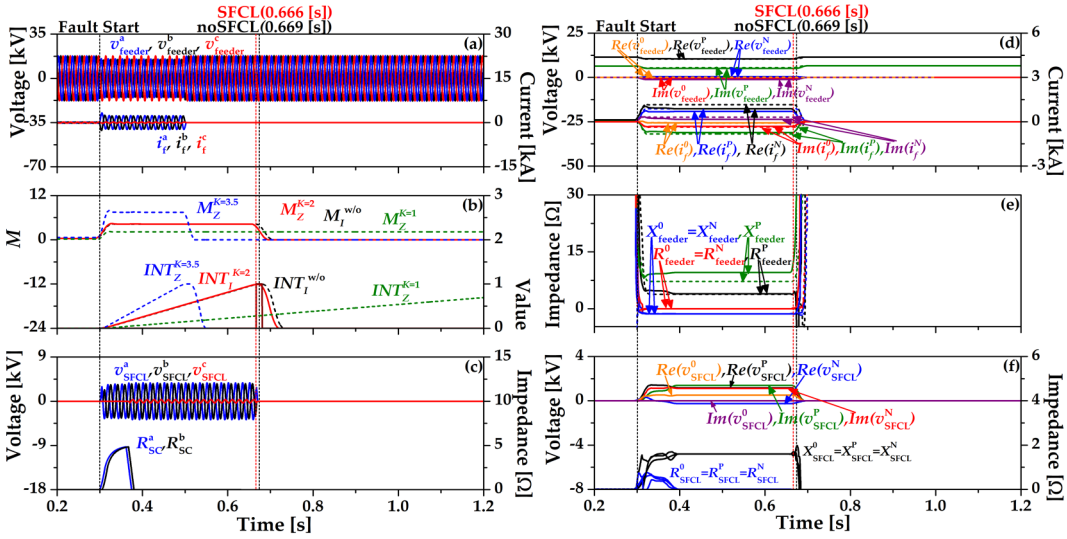

Figure 7. Waveforms and signals of OCR using M_I, M_Z in DLG. (**a**) Three phase feeder voltage (v_{feeder}), current (i_f). (**b**) Index of CB (M_I, M_Z) and signal of OCR (INT_I, INT_Z). (**c**) Three phase SFCL voltage (v_{SFCL}), HTSC element (R^a_{SC}, R^b_{SC}). (**d**) Sequence feeder voltages (v^0_{feeder}, v^P_{feeder}, v^N_{feeder}), sequence feeder currents (i^0_f, i^P_f, i^N_f). (**e**) Sequence feeder impedances (R^0_{feeder}, R^P_{feeder}, R^N_{feeder}, X^0_{feeder}, X^P_{feeder}, X^N_{feeder}). (**f**) Sequence SFCL voltages (v^0_{SFCL}, v^P_{SFCL}, v^N_{SFCL}) and sequence SFCL impedances (R^0_{SFCL}, R^P_{SFCL}, R^N_{SFCL}, X^0_{SFCL}, X^P_{SFCL}, X^N_{SFCL}).

4.3. Triple-Line Ground Fault

Figure 8 shows the triple-line ground fault (TLG) using the existing over-current relay (OCR) algorithm (2). OCR operates at 0.627 [s] without the SFCL and OCR with SFCL operates at 0.757 [s]. Figure 8a shows the feeder voltages and currents when the SFCL is installed. The operation of OCR using (2) is expressed in the integration value INT_I, which increases after the fault occurs and when INT_I approaches "1" point as seen in Figure 8b. In Figure 8c, the HTSC element (R^a_{SC}, R^b_{SC}, R^c_{SC}) gets the resistance value because the fault current (I_f) exceeds the critical current and R^a_{SC}, R^b_{SC}, R^c_{SC} become zero when the breaker in the SFCL is operated, as explained in Section 2.2. During the fault time, the voltage of the SFCL (v_{SFCL}) is reduced by R^a_{SC}, R^b_{SC}, R^c_{SC} and increased again since the direction of the fault current changes to the current limiting reactor (CLR). Figure 8d shows the sequence components waveforms of the feeder voltages and currents. The dotted line is the feeder voltages and currents using the existing OCR algorithm (2) without the SFCL and the solid line is the identical condition with the SFCL. Figure 8e is the sequence components' waveforms of feeder impedances. The dotted line is the feeder impedances using existing the OCR algorithm (2) without the SFCL and the solid line is the identical condition with the SFCL. Figure 8f is the sequence component waveforms of the SFCL voltages and impedances. Unlike the results of the unbalanced faults (SLG, DLC), the zero and negative sequences are nonexistent.

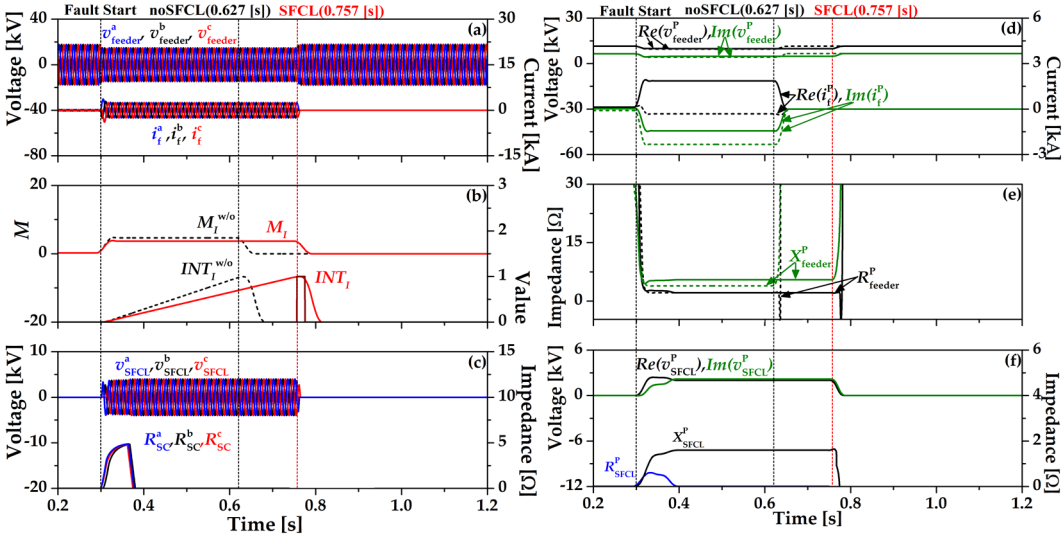

Figure 8. Waveforms and signals of OCR using M_I in TLG. (**a**) Three phase feeder voltage (v_{feeder}), current (i_f). (**b**) Index of CB (M_I) and signal of OCR (INT_I). (**c**) Three phase SFCL voltage (v_{SFCL}), HTSC element (R^a_{SC}, R^b_{SC}, R^c_{SC}). (**d**) Positive sequence feeder voltage (v^P_{feeder}), positive sequence feeder current (i^P_f). (**e**) Sequence feeder impedances (R^P_{feeder}, X^P_{feeder}). (**f**) Positive sequence SFCL voltage (v^P_{SFCL}) and positive SFCL impedance (R^P_{SFCL}, X^P_{SFCL}).

Figure 9 shows the triple-line ground fault (TLG) using the impedance compensation method (17). In Figure 7b, the operation of OCR using (17) is expressed in the integration value INT_Z, which has three different waveforms depending on the K value (1, 2, 3.5). When $K = 1$, index value (M_Z) and INT_Z are most similar to the existing OCR algorithm (2) without SFCL ($INT^{w/o}_I$). OCR operates at 0.626 [s] and decreased by 0.13 [s] compared to existing OCR algorithm (2) with SFCL. In Figure 9c, resistance of HTSC element (R^a_{SC}, R^b_{SC}, R^c_{SC}) is the same as Figure 6 since the breaker operation is constant since the critical current (I_C) is maintained. During the fault time, voltage of the SFCL (v_{SFCL}) is reduced by R^a_{SC}, R^b_{SC}, R^c_{SC} and increased again since the direction of the fault current changes to the current limiting reactor (CLR). Figure 9d shows the sequence components waveforms of the feeder voltages and currents. The dotted line is the feeder voltages and currents using the existing OCR algorithm (2) without the SFCL and the solid line is the impedance compensation method (17) with the SFCL. Figure 9e is the sequence components' waveforms of feeder impedances. The dotted line is the feeder impedances using the existing OCR algorithm (2) without the SFCL and the solid line is the impedance compensation method (17) with the SFCL. Figure 9f is the sequence component waveforms of the SFCL voltages and impedances. Unlike the results of the unbalanced faults (SLG, DLC), the zero and negative sequences are nonexistent.

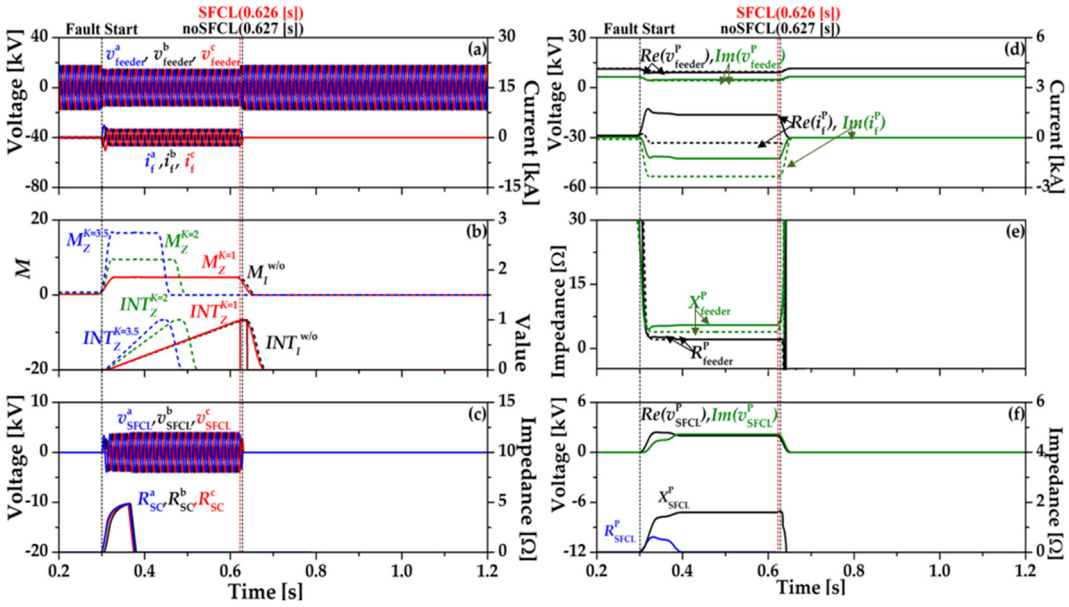

Figure 9. Waveforms and signals of OCR using M_I, M_Z in TLG. (**a**) Three phase feeder voltage (v_{feeder}), current (i_f). (**b**) Index of CB (M_I, M_Z) and signal of OCR (INT_I, INT_Z). (**c**) Three phase SFCL voltage (v_{SFCL}), HTSC element (R^a_{SC}, R^b_{SC}, R^c_{SC}). (**d**) Positive sequence feeder voltage (v^P_{feeder}), positive sequence feeder current (i^P_f). (**e**) Positive sequence feeder impedance (R^P_{feeder}, X^P_{feeder}). (**f**) Positive sequence SFCL voltage (v^P_{SFCL}) and positive sequence SFCL impedance (R^P_{SFCL}, X^P_{SFCL}).

5. Discussion

The simulations are proposed in operation characteristics of OCR with SFCL depending on the three types of ground faults. In order to improve the trip delay of OCR, the existing OCR algorithm (2) changes into the impedance compensation method (17) by substituting the sequence components of a power distribution system. It is confirmed that the impedance compensation method improves the trip time delay of OCR in all ground fault types. Impedance compensation method (17) K should be set differently because the index value and trip time are different in three types of ground faults. Table 4 shows the proper K value, trip time of existing OCR algorithm and trip time of impedance compensation method according to the ground fault type.

Table 4. Simulation result by fault type.

Fault Type	K	Existing OCR Algorithm [s]	Impedance Compensation Method [s]
SLG	3.5	0.882	0.88
DLG	2	0.669	0.666
TLG	1	0.627	0.626

6. Conclusions

The proper operation of OCR with SFCL is the impedance compensation method which has been introduced to improve the trip time delay of OCR in three types of ground faults. In case of the different fault types, the impedance compensation method is distinguished according to the compensation constant. The impedance components of the impedance compensation method are derived from voltages and currents of a power distribution system.

From the simulation results comparing the existing OCR algorithm and the impedance compensation method in three types of ground faults, the latter one improves the trip time delay of OCR due to the SFCL while the fault current is reduced. To apply to all types of ground fault, the compensation constant of the impedance compensation method should be changed.

In the future research, the protection coordination of OCRs using the impedance compensation method in unbalanced fault situation, considering dispersed generation in a power distribution system, will be studied with more elaborate compensation constants.

Author Contributions: Supervision, S.-H.L.; Writing—original draft, Y.-J.C.; Writing—review & editing, S.-H.L. All authors have read and agreed to the published version of the manuscript.

Funding: This work was supported by Korea Institute for Advancement of Technology (KIAT) grant funded by Korea Government(MOTIE) (P0017033, The Competency Development Program for Industry Specialist) and was also supported by the National Research Foundation of Korea (NRF) grant funded by the Korea government (MOE) (No. 2020R1F1A1077206).

Data Availability Statement: Data is contained within the article.

Conflicts of Interest: The authors declare no conflict of interest.

References

1. Kim, H.J.; Yoon, T.A. Study on application of a high-speed trigger-type SFCL (TSFCL) for interconnection of power systems with different reliabilities. *IEEE Trans. Appl. Supercond.* **2010**, *20*, 1194–1198.
2. Song, M.; Tang, Y.; Zhou, Y.; Ren, L.; Chen, L.; Cheng, S. Electromagnetic Characteristics Analysis of Air-Core Transformer Used in Voltage Compensation Type Active SFCL. *IEEE Trans. Appl. Supercond.* **2010**, *20*, 1194–1198.
3. Zou, Z.-C.; Chen, X.-Y.; Li, C.-S.; Xiao, X.Y.; Zhang, Y. Conceptual Design and Evaluation of a Resistive-Type SFCL for Efficient Fault Ride through in a DFIG. *IEEE Trans. Appl. Supercond.* **2016**, *26*, 7.
4. Lim, S.H.; Han, T.H.; Cho, Y.S.; Choi, H.S.; Han, B.S.; Lee, S.W. Quench characteristics of HTSC elements in integrated three-phase flux-lock type SFCL according to ground-fault types. *Phys. C Supercond. Appl.* **2007**, *463*, 1198–1203.
5. Hyun, O.-B.; Park, K.-B.; Sim, J.; Kim, H.-R.; Yim, S.-W.; Oh, I.-S. Introduction of a Hybrid SFCL in KEPCO Grid and Local Points at Issue. *IEEE Trans. Appl. Supercond.* **2009**, *19*, 1946–1949.
6. Shirai, Y.; Noda, S.; Yamabe, K.; Hattori, K.; Baba, J.; Nishihara, T.; Nitta, T.; Kobayashi, S.; Sato, K. Current Limiting Performance of Three-Phase Concentric Transformer Type SFCL at Unbalanced Fault Conditions. *IEEE Trans. Appl. Supercond.* **2012**, *23*, 5601905.
7. Kim, W.-S.; Hyun, O.-B.; Park, C.-R.; Yim, S.-W.; Yu, S.-D.; Yang, S.-E.; Kim, H.-S.; Kim, H.R. Dynamic Characteristics of a 22.9 kV Hybrid SFCL for Short-Circuit Test Considering a Simple Coordination of Protection System in Distribution Networks. *IEEE Trans. Appl. Supercond.* **2012**, *22*, 3.
8. Sung, B.C.; Park, D.K.; Park, J.W.; Ko, T.K. Study on a Series Resistive SFCL to Improve Power System Transient Stability: Modeling, Simulation, and Experimental Verification. *IEEE Trans. Ind. Electronics* **2009**, *56*, 2412–2419.
9. Shen, B.; Chen, Y.; Li, C.; Wang, S.; Chen, X. Superconducting fault current limiter (SFCL): Experiment and the simulation from finite-element method (FEM) to power/energy system software. *Energies* **2021**, *234*, 1.
10. Huh, J.-S.; Shin, H.-S.; Moon, W.-S.; Kang, B.-W.; Kim, J.-C. Study on Voltage Unbalance Improvement Using SFCL in Power Feed Network with Electric Railway System. *IEEE Trans. Appl. Supercond*. **2013**, *23*, 3601004.
11. Choi, H.-Y.; Cho, Y.-S.; Jung, B.-I.; Chung, D.-C.; Fathy, A. Comparison of the Unbalanced Faults in Three-Phase Resistive and Matrix-Type SFCLs. *IEEE Trans. Appl. Supercond*. **2010**, *20*, 1215–1218.
12. Lim, S.-H.; Lim, S.-T. Current Limiting and Recovery Characteristics of a Trigger-Type SFCL Using Double Quench. *IEEE Trans. Appl. Supercond.* **2018**, *28*, 17572499.
13. Martini, L.; Bocchi, M.; Angeli, G.; Ascade, M.; Rossi, V.; Valzasina, A.; Ravetta, C.; Fratti, S.; Martino, E. Live grid field-testing final results of the first Italian superconducting fault current limiter and severe 3-phase fault experience. *IEEE. Trans. Appl. Supercond.* **2015**, *25*, 3.
14. Shin, J.W.; Kim, J.C.; Lee, H.; Yoon, K.H.; Chai, H.S.; Kim, J.S. Impact of SFCL according to Voltage Sags Based Reliability. *IEEE Trans. Appl. Supercond.* **2021**, *31*, 5.
15. Lim, S.T.; Lim, S.H. Analysis on operational improvement of OCR using voltage component in a power distribution system for application of SFCL. *J. Electr. Eng. Technol*. **2019**, *14*, 1027–1033.
16. Park, M.-K.; Lim, S.-H. Impedance Compensation Method of Protective Relay for SFCL's Application in a Power Distribution System. *IEEE Trans. Appl. Supercond.* **2021**, *31*, 20463141.
17. Park, M.-K.; Lim, S.-H. Analysis on Protection Coordination of OCRs Using Voltage Components for the Application of SFCL in a Power Distribution System with DG. *IEEE Trans. Appl. Supercond.* **2021**, *31*, 20994711.
18. Moon, J.; Lim, S.; Kim, J.; Yun, S. Assessment of the Impact of SFCL on Voltage Sags in Power Distribution System. *IEEE Trans. Appl. Supercond.* **2011**, *21*, 2161–2164.
19. Lim, S.T.; Lim, S.H. Analysis on protective coordination between over-current relays with voltage component in a power distribution system with SFCL. *IEEE Trans. Appl. Supercond*. **2020**, *30*, 4.
20. Choi, S.-J.; Lim, S.H. Enhancement on the Fault Ride through Capability of Power Distribution Systems Linked by Distributed Generation due to the Impedance of Superconducting Fault Current Limiters. *Energies* **2019**, *12*, 4810.

21. Lim, S.T.; Lim, S.H. Study on improvement of overcurrent relay (OCR)'s operation due to application of superconducting fault current limiter (SFCL) in power distribution system with a dispersed generation. *Trans. Korean Inst. Electr. Eng*. **2017**, *66*, 300–304.
22. Mangunkusumo, K.G.H.; Kusuma, A.A.; Munir, B.S. A Case Study of Mutual Impedance Effect in Parallel Transmission Lines Under Maintenance Condition. In Proceedings of the 2018 10th International Conference on Information Technology and Electrical Engineering (ICITEE), Bali, Indonesia, 24–26 July 2018; pp. 192–195.
23. Koirala, A.; D'hulst, R.; van Hertem, D. Impedance modelling for European style Distribution Feeder. In Proceedings of the 2019 International Conference on Smart Energy Systems and Technologies (SEST), Porto, Portugal, 11 September 2019.
24. Wen, B.; Burgos, R.; Boroyevich, D.; Mattavelli, P.; Shen, Z. AC Stability Analysis and dq Frame Impedance Specifications in Power-Electronics-Based Distributed Power Systems. *IEEE J. Emerg. Sel. Top. Power Electron.* **2017**, *5*, 1455–1465.
25. Saadat, H. *Power System Analysis*; Milwaukee School of Engineering: Milwaukee, WI, USA, 1999.
26. Sravya, A.S.L.; Yoshita, L.N.; Reddy, B.D.D.; Sailaja, V.; Manitha, P.V.; Deepa, K. Impedance Bus Matrix Formation using Bus Building Algorithm for Power System Analysis. In Proceedings of the 2020 IEEE International Women in Engineering (WIE) Conference on Electrical and Computer Engineering (WIECON-ECE), Bhubaneswar, India, 26–27 December 2020; pp. 200–205.
27. Paz, M.C.R.; Ferraz, R.G.; Bretas, A.S.; Leborgne, R.C. System unbalance and fault impedance effect on faulted distribution networks. *Comput. Math. Appl.* **2010**, *60*, 1105–1114.
28. Korea Electric Power Corporation. *Distribution Practical III*; Korea Electric Power Corporation: Seoul, Korea, 2006.